0026-895X/98/010129-10$3.00/0
Copyright © by The American Society for Pharmacology and Experimental Therapeutics
All rights of reproduction in any form reserved.
MOLECULAR PHARMACOLOGY, **54:**129–138 (1998).

MOLECULAR PHARMACOLOGY

# Ligand Specificity of the Genetic Variants of Human $\alpha_1$-Acid Glycoprotein: Generation of a Three-Dimensional Quantitative Structure-Activity Relationship Model for Drug Binding to the A Variant

FRANÇOISE HERVÉ, GIULIA CARON, JEAN-CLAUDE DUCHÉ, PATRICK GAILLARD, NOORSAADAH ABD. RAHMAN,[1] ANNA TSANTILI-KAKOULIDOU, PIERRE-ALAIN CARRUPT, PHILIPPE D'ATHIS, JEAN-PAUL TILLEMENT, and BERNARD TESTA

*Service Hospitalo-Universitaire de Pharmacologie de Paris XII, Centre Hospitalier Intercommunal de Créteil, F-94010 Créteil Cedex, France (F.H., J.-C.D., J.-P.T.), Institut de Chimie Thérapeutique Section de Pharmacie, Université de Lausanne, CH-1015 Lausanne-Dorigny, Switzerland (G.C., P.G., N.A.R., A.T.-K., P.-A.C., B.T.), and Laboratoire d'Informatique Médicale, Faculté de Médecine de Dijon, F-21033 Dijon Cedex, France (P.d'A.)*

Received August 1, 1997; Accepted March 16, 1998

This paper is available online at http://www.molpharm.org

## ABSTRACT

Human $\alpha_1$-acid glycoprotein (AAG) is a mixture of at least two genetic variants: the A variant and the F1 and/or S variant or variants, which are encoded by two different genes. In a continuation of previous studies indicating specific drug transport roles for each AAG variant according to its separate genetic origin, this work was designed to (1) determine the affinities of the two main gene products of AAG (i.e., the A variant and a mixture of the F1 and S variants) for 35 chemically diverse drugs and (2) to obtain meaningful 3D-QSARs for each binding site. Affinities were obtained by displacement experiments, leading to qualitative indications about binding site characteristics. In particular, drugs binding selectively to the A variant displayed some common structural features, but this was not seen for the F1*S variants. Three-dimensional QSAR analyses using the CoMFA method yielded a steric model for binding to the A variant, from which a simplified haptophoric model was derived. In contrast, no statistically sound model was found for the F1*S variants, possibly due (among other reasons) to an insufficient number of high affinity ligands in the set.

AAG is a protein whose heterogeneity has significant effects on drug transport; it is the main carrier of basic drugs and other ligands in plasma (Kremer *et al*., 1988). AAG exists as a mixture of two or three genetic variants (i.e., the A variant and the F1 and/or S variants) in the plasma of most individuals (Eap and Baumann, 1989; Yuasa *et al*., 1993). The AAG polymorphism is explained by the presence of two different genes coding for the protein (Dente *et al*., 1987), of which the *AAG-A* gene encodes the F1 and S variants and the *AAG-B*/*B′* gene encodes the A variant (Tomei *et al*., 1989). The *AAG-B*/*B′* gene is structurally similar to the *AAG-A* gene but contains 22 base substitutions. Accordingly, the A variant and the F1*S variants should differ in their amino acid sequences by (at least) 22 residues, among a total of 181 residues (Schmid, 1975). In addition, the F1 and S variants encoded by two alleles of the *AAG-A* gene (Yuasa *et al*., 1993) should differ by only a few amino acids (less than five) (Dente *et al*., 1987).

Recently, a fractionation method was developed for the AAG variants (Hervé *et al*., 1992, 1993a), and it was used on a preparative scale to purify large amounts of the A variant and of a mixture of the F1 and S variants. The source was a commercial AAG of human origin containing similar proportions of the three variants. Large differences in the binding of various drugs have been demonstrated between the A and F1*S variants, indicating specific drug transport roles for each AAG variant, according to their separate genetic origin (Hervé *et al*., 1993b, 1996).

AAG is an important determinant of the plasma binding of

B.T. and P.A.C. are indebted to the Swiss National Science Foundation for support. F.H., J.C.D., and J.P.T. are indebted to the Ministère de l'Education Nationale (EA 427) and to the Réseau de Pharmacologie Clinique for support. N.A.R. acknowledges receipt of a JWT Jones Travelling Fellowship given by the Royal Society of Chemistry. A.T.K. is indebted to the Foundation Herbette (University of Lausanne) for a travel grant. F.H. and G.C. contributed equally to this study.

[1] Current affiliation: Department of Chemistry, University of Malaya, 50603 Kuala Lumpur, Malaysia.

**ABBREVIATIONS:** AAG, human $\alpha_1$-acid glycoprotein; CoMFA, comparative molecular field analysis; DISCO, distance comparison; PLS, partial least squares; QSAR, quantitative structure-activity relationships; SAMPLS, sample-distance partial least squares; 3D-QSAR, three-dimensional quantitative structure-activity relationships.



Downloaded from molpharm.aspetjournals.org at ASPET Journals on November 19, 2017

many basic drugs (Routledge, 1986). In this context, the existence of functional heterogeneity between the AAG variants, together with variable concentrations of these variants between individuals (Eap *et al.*, 1990), could be responsible for interindividual differences in drug binding, such as those reported by some investigators (Tinguely *et al.*, 1985; Eap *et al.*, 1990). Changes in the expression of the genetic variants of AAG during inflammation (Eap *et al.*, 1991) or illness might also result in altered plasma drug binding. Finally, the drug binding differences demonstrated between the A and the F1*S variants indicate that AAG, considered as a single protein, would present not one but at least two separate and fractional drug binding sites with different binding specificities. In addition, because the A-to-F1*S variant ratio varies among individuals, so would the proportions of these sites. The fact that some drugs are bound only by one of these sites might result in a binding lower than expected from the total AAG concentration and in an increased risk of drug interactions due to higher site occupancy.

Given the potential clinical and biological significance of AAG polymorphism, it would be useful to gain insight into the nature and topography of the binding site or sites likely to be present on each AAG variant, with the ultimate goal of predicting affinities and anticipating possible risk factors. Hence, the first objective of this work was to improve our understanding of the binding specificity of the AAG variants using a variety of drugs belonging to different pharmacological and chemical classes. To this end, displacement experiments were performed using [$^3$H]imipramine and [$^{14}$C]warfarin as selective and high affinity ligands for the A and F1*S variants, respectively. In the second part of the work, the binding data collected here and previously (Hervé *et al.*, 1996) were used in a 3D-QSAR analysis using CoMFA, with the objective of obtaining a three-dimensional model of the binding sites.

## Experimental Procedures

### Materials

The A variant and a mixture of the F1 and S variants in the native (sialylated) form were separated by chromatography from commercial preparations of human AAG [from Cohn Fraction VI; Sigma Chemical, St. Louis, MO (batches 90H9317 and 13H9336], as described previously (Hervé *et al.*, 1992, 1993a). The proportions of the F1, S, and A variants in commercial AAG preparations are nearly constant (~40%, ~30%, and ~30%, respectively) (Hervé *et al.*, 1997). After chromatography, >95% of each variant was recovered. The composition of the isolated variants was checked by polyacrylamide gel isoelectric focusing (Eap and Baumann, 1988), after small amounts of the different samples had been desialylated with neuraminidase (Hervé *et al.*, 1993b). The F1*S mixture consisted of ~60% F1 and ~40% S, as determined by laser densitometry. It also contained trace amounts (<4%) of the A variant. The A variant sample was devoid of any F1*S variants. To remove possible endogeneous inhibitors, the AAG variant samples were treated with charcoal, pH 7.4, as described previously (Hervé *et al.*, 1993b).

[$^3$H]Imipramine (25 Ci/mmol, 925 Gbq/mmol) and [$^{14}$C]warfarin (46 mCi/mmol, 1.70 Gbq/mmol) were purchased from Amersham International (Buckinghamshire, UK). The radiochemical purity of the drugs was >98% by thin layer chromatography. Binedaline was a gift from Cassenne (Paris-La Défense, France). Bornaprolol was a gift from Rhône-Poulenc Rorer (Neuilly/Seine, France). Imipramine, desipramine, and clomipramine were gifts from from Ciba-Geigy (Rueil-Malmaison, France). Isradipine was a gift from Sandoz (Basel, Switzerland). Minaprine was a gift from Clin Midy-Sanofi (Paris, France). Propafenone was a gift from Knoll France (Levallois-Perret, France). Tertatolol was a gift from Servier (Jidy, France). Cetirizine was a gift from UCB Pharma France S.A. (Nanterre, France). Desmethylclomipramine was a gift from Dr. C. B. Eap (University Psychiatric Hospital, Prilly-Lausanne, Switzerland). Amitriptyline, auramine O, capsaicin (8-methyl-*N*-vanillyl-6-nonenamide), chlorpheniramine, diazepam, diphenhydramine, chlorcyclizine, maprotiline, nortriptyline, prazosin, promethazine, (*rac*)-propranolol, (*S*)-(-)propranolol, (*R*)-(+)-propranolol, pyrilamine maleate, quinidine, thioridazine, trazodone, viloxazine, and warfarin were purchased from Sigma.

### Binding Experiments

**Methods.** AAG concentrations of the charcoal-extracted A and F1*S variant samples were measured by an immunonephelometric method, with a Beckman assay kit and apparatus (model 7571, ARRAY TM Protein System; Beckman Instruments, Fullerton, CA). To calculate the molar concentration of AAG, a molecular mass of 40,000 kDa was assumed (Kremer *et al.*, 1988).

All solutions were prepared in 67 mM sodium/potassium phosphate buffer, pH 7.4, containing 50 or 150 mg/liter gelatin depending on the marker ligand used. Gelatin was used to avoid ligand adsorption to dialysis cells or membranes (Visking 18/32; Union Carbide, Chicago, IL). Its use has proved to be effective for avoiding the nonspecific adsorption of compounds **1**, **2**, **9**, **10**, **15**, **18**, **24**, **30**, and **33** described in Table 1. When necessary, the ligands were dissolved in a small volume of ethanol or methanol (grade A; Merck, Darmstadt, Germany) (final concentration, <2%).

Competitive binding experiments were performed by equilibrium dialysis at 4° and pH 7.4 using dialysis cells of 100 $\mu$l half-cell volume, as described previously (Hervé *et al.*, 1996). Dialysis time was 22–24 hr, depending on the ligand, with gentle shaking. Preliminary tests with various ligands gave identical binding results for 22 and 30 hr incubations (not shown), showing that equilibrium had been reached by 22 hr without significant protein denaturation. The final concentrations of charcoal-extracted A and F1*S variants in the protein half-cells were 10 $\mu$M. The concentration of marker ligands, imipramine, and warfarin in the ligand half-cells was 2 $\mu$M (approximately the high affinity dissociation constant for each marker on the corresponding AAG variant; Hervé *et al.*, 1993b), with a constant amount of radioactivity (0.99 kBq for [$^3$H]imipramine or 0.135 kBq for [$^{14}$C]warfarin). Displacing ligand concentrations covered the range 1:1 to 100:1 [inhibitor]/[marker] except for capsaicin and thioridazine, for which the ratios did not exceed 60:1 and 50:1, respectively, because of their low aqueous solubility. Each inhibitor was examined at 8–19 different concentrations. In the absence of inhibitor, the protein-bound concentration of marker was 1.59 $\pm$ 0.10 $\mu$M for imipramine with the A variant and 1.67 $\pm$ 0.11 $\mu$M for warfarin and the F1*S variants (>84); these values served as controls. After equilibration, the concentrations of labeled marker ligand in 50-$\mu$l samples from each half-cell were measured by liquid scintillation counting with a Packard Tricarb 2200 CA counter and Picofluor 40 as scintillant (Packard, Downers Grove, IL). The bound (B) molar concentration of the labeled ligand was calculated.

**Evaluation of the displacement data.** Two different expressions of a model for the competitive inhibition of the marker (imipramine or warfarin) binding by displacer were used to analyze the displacement data, to determine (1) the ligand inhibitory potencies ($IC_{50}$) and (2) the ligand association constants (here abbreviated $K'$) for binding to each AAG variant. Each parameter was estimated with its standard deviation by nonlinear regression analysis using a Gauss-Newton algorithm.

**Determination of the $IC_{50}$ parameter.** The relationship between the percentage displacement of the respective marker by an

Downloaded from molpharm.aspetjournals.org at ASPET Journals on November 19, 2017

inhibitor and the concentration of the inhibitor was modeled with eq. 1, assuming a pseudo-Hill coefficient of 1:

$$\% \text{ displacement} = 1 - \frac{B}{B_{max}} = 1 - \frac{1}{\left(1 + \frac{I_f}{IC_{50}}\right)} \quad (1)$$

where $B$ is the concentration of bound marker measured at equilibrium for each free concentration of inhibitor ($I_f$), $B_{max}$ is the maximum concentration of bound marker measured at equilibrium in the absence of inhibitor (i.e., $B = B_{max}$ when $I_f = 0$), and $IC_{50}$ is the theoretical molar concentration of the inhibitor producing a 50% decrease in $B_{max}$.

The $IC_{50}$ value of each inhibitor was estimated from measurements of $B$ as a function of $I_f$, with the latter concentration being approximated by the total concentration of inhibitor ($I_t$).

**Determination of the $K'$ parameter.** These equations were used to determine the association constant ($K'$) of each inhibitor (Hervé *et al*., 1996):

$$B = K_a \cdot (nP_t - I_b - B) \cdot (T - B) \quad (2)$$

TABLE 1
Ligand inhibitory potencies ($IC_{50}$) and binding association constant ($K'$) to the separate AAG variants

| Inhibitor[a] | Ligand inhibitory potencies ($IC_{50}$)[b] | | Ligand binding association constant ($K'$) | | |
|---|---|---|---|---|---|
| | A variant | F1*S variants | A variant | F1*S variants | Selectivity[d] |
| | *μM* | | *×10⁶ liters/mol* | | |
| Analgesic drugs | | | | | |
| Methadone (**1**) | 14.2 ± 0.3 | [c] | 0.994 ± 0.090[e] | [ce] | [c] |
| Anticoagulant drugs | | | | | |
| Warfarin (**2**) | [c] | 10.7 ± 0.1 | [c] | 1.921 ± 0.120[e] | [c] |
| Antihistaminic drugs | | | | | |
| Cetirizine (**3**) | 377 ± 10 | 553 ± 15 | 0.025 ± 0.067 | 0.025 ± 0.081 | 1.0 |
| Chlorcyclizine (**4**) | 123 ± 2 | 525 ± 12 | 0.076 ± 0.055 | 0.026 ± 0.056 | 2.9 |
| Chlorpheniramine (**5**) | 412 ± 9 | 589 ± 20 | 0.023 ± 0.069 | 0.024 ± 0.078 | 1.0 |
| Diphenhydramine (**6**) | 37.8 ± 0.4 | 404 ± 7 | 0.270 ± 0.070 | 0.033 ± 0.041 | 8.2 |
| Promethazine (**7**) | 18.0 ± 0.4 | 181 ± 5 | 0.633 ± 0.110 | 0.071 ± 0.061 | 9.0 |
| Pyrilamine (**8**) | 260 ± 7 | 271 ± 8 | 0.035 ± 0.086 | 0.048 ± 0.079 | 0.7 |
| Cardiovascular drugs | | | | | |
| Antiarrhythmics | | | | | |
| Disopyramide (**9**) | 8.1 ± 0.2 | [c] | 2.510 ± 0.090[e] | [ce] | [c] |
| Lidocaine (**10**) | 175 ± 3 | 511 ± 18 | 0.055 ± 0.053[e] | 0.027 ± 0.090[e] | 2.0 |
| Propafenone (**11**) | 5.6 ± 0.1 | 51.1 ± 0.8 | 4.180 ± 0.190 | 0.271 ± 0.050 | 15.4 |
| Quinidine (**12**) | 76.1 ± 1.8 | 99.9 ± 2.4 | 0.125 ± 0.065 | 0.135 ± 0.097 | 0.9 |
| Antihypertensive drugs | | | | | |
| $\alpha_1$ Blockers | | | | | |
| Prazosin (**13**) | 479 ± 21 | 107 ± 2 | 0.020 ± 0.074 | 0.121 ± 0.084 | 0.17 |
| $\beta$ Blockers | | | | | |
| Bornaprolol (**14**) | 9.3 ± 0.7 | 10.3 ± 0.4 | 2.040 ± 0.095 | 2.080 ± 0.076 | 1.0 |
| Propranolol (**15**) | 56.9 ± 1.0 | 95.5 ± 1.8 | 0.170 ± 0.090 | 0.142 ± 0.080 | 1.2 |
| (*S*)-Propranolol | 52.1 ± 0.1 | 94.0 ± 1.8 | 0.190 ± 0.060 | 0.142 ± 0.079 | 1.3 |
| (*R*)-Propranolol | 100 ± 2 | 88.7 ± 1.6 | 0.093 ± 0.044 | 0.153 ± 0.080 | 0.6 |
| Tertatolol (**16**) | 10.1 ± 0.2 | 15.5 ± 0.4 | 1.610 ± 0.148 | 1.137 ± 0.093 | 1.4 |
| Calcium channel blockers | | | | | |
| Isradipine (**17**) | 17.7 ± 0.8 | 24.3 ± 0.7 | 0.768 ± 0.089 | 0.653 ± 0.062 | 1.2 |
| Vasodilatator drugs | | | | | |
| Dipyridamole (**18**) | 63.0 ± 1.2 | 9.0 ± 0.2 | 0.156 ± 0.066[e] | 2.648 ± 0.080[e] | 0.06 |
| Psychotropic drugs | | | | | |
| Antidepressants | | | | | |
| Amitriptyline (**19**) | 6.1 ± 0.2 | 176 ± 3 | 3.370 ± 0.200 | 0.074 ± 0.072 | 45.5 |
| Binedaline (**20**) | 17.0 ± 0.6 | 5.9 ± 0.3 | 0.786 ± 0.087 | 4.620 ± 0.080 | 0.17 |
| Clomipramine (**21**) | 23.4 ± 1.0 | 65.6 ± 3.5 | 0.489 ± 0.045 | 0.196 ± 0.100 | 2.5 |
| Desipramine (**22**) | 47.3 ± 0.9 | 814 ± 33 | 0.211 ± 0.080 | 0.018 ± 0.050 | 11.7 |
| Desmethylclomipramine (**23**) | 41.7 ± 0.7 | 183 ± 3 | 0.247 ± 0.068 | 0.072 ± 0.044 | 3.4 |
| Imipramine (**24**) | 15.0 ± 0.3 | 159 ± 4 | 0.940 ± 0.120[e] | 0.080 ± 0.067 | 11.8 |
| Maprotiline (**25**) | 62.6 ± 1.2 | [c] | 0.159 ± 0.050 | [c] | [c] |
| Nortriptyline (**26**) | 14.8 ± 0.4 | 407 ± 15 | 0.898 ± 0.117 | 0.033 ± 0.096 | 27.2 |
| Trazodone (**27**) | 67.5 ± 1.4 | 55.0 ± 0.9 | 0.141 ± 0.066 | 0.252 ± 0.064 | 0.6 |
| Viloxazine (**28**) | 361 ± 7 | 191 ± 2 | 0.026 ± 0.056 | 0.069 ± 0.052 | 0.4 |
| Anxiolytics | | | | | |
| Diazepam (**29**) | 181 ± 3 | 403 ± 130 | 0.051 ± 0.074 | 0.033 ± 0.055 | 1.5 |
| Neuroleptics | | | | | |
| Chlorpromazine (**30**) | 14.0 ± 0.4 | 18.0 ± 0.5 | 0.970 ± 0.110[e] | 0.958 ± 0.078[e] | 1.0 |
| Thioridazine (**31**) | 6.1 ± 0.1 | 5.0 ± 0.1 | 4.020 ± 0.090 | 6.000 ± 0.100 | 0.7 |
| Psychotropics | | | | | |
| Minaprine (**32**) | 673 ± 18 | 309 ± 9 | 0.015 ± 0.061 | 0.043 ± 0.087 | 0.3 |
| Steroids | | | | | |
| Progesterone (**33**) | 59.2 ± 1.1 | 91.9 ± 2.2 | 0.165 ± 0.056[e] | 0.146 ± 0.055[e] | 1.1 |
| Miscellaneous | | | | | |
| Auramine O (**34**) | 327 ± 16 | 458 ± 11 | 0.029 ± 0.120 | 0.029 ± 0.069 | 1.0 |
| Capsaicin (**35**) | 26.7 ± 0.6 | 42.0 ± 0.5 | 0.400 ± 0.110 | 0.343 ± 0.053 | 1.2 |

The two parameters $IC_{50}$ and $K'$ were derived by different mathematical methods (see Materials and Methods).

[a] The numbers indicated for the ligands correspond to those cited in the text.

[b] The $IC_{50}$ values correspond to the micromolar concentration of the inhibitors producing a 50% decrease of [$^3$H]imipramine (A variant) or [$^{14}$C]warfarin (F1*S variants) binding.

[c] No $IC_{50}$ and $K'$ values could be calculated because the displacement data showed important deviations from theoretical curves representing a competitive inhibition of the marker binding by displacer.

[d] The selectivity factor corresponds to the affinity ratio of A over F1*S.

[e] Determined in a previous study [Hervé *et al.,* 1996] using the same equilibrium dialysis method and the same experimental conditions.

Downloaded from molpharm.aspetjournals.org at ASPET Journals on November 19, 2017

$$I_b = K' \cdot (nP_t - I_b - B) \cdot (I_t - I_b) \quad (3)$$

where n and $K_a$ are the number of high affinity binding sites and the association constant for the marker ligand, respectively; $B$ and T are the bound and total concentrations of the marker ligand; $I_b$ and $I_t$ are the bound and total concentrations of the inhibitor; and $P_t$ is the concentration of the protein. These equations can be resolved to eliminate the unknown concentration $I_b$.

The inhibitor association constant ($K'$) was calculated from measurements of B expressed as a function of the total concentration of the inhibitor ($I_t$).

On the basis of the individual binding parameters for the markers determined and discussed previously ($n_1 = 0.71$ and $k_1 = 0.98 \times 10^6$ liter/mol, $n_2 = 1.72$ and $k_2 = 1.86 \times 10^4$ liter/mol for imipramine binding to the A variant, and $n_1 = 0.58$ and $k_1 = 1.89 \times 10^6$ liter/mol, $n_2 = 0.52$ and $k_2 = 1.59 \times 10^4$ liter/mol for warfarin binding to the F1*S variants) (Hervé *et al.*, 1993b), theoretical calculations showed that the high affinity binding site of the markers to their respective AAG variants in the absence of inhibitor represented >94% of the total protein binding of each marker. Accordingly, the low affinity binding sites were not taken into account here. In addition, the calculations showed that binding of each marker to the corresponding AAG variant would be linear at the experimental concentration used for each marker.

### CoMFA Study

**Binding data.** Input data (dependent variables) were $pIC_{50}$ values (i.e., minus the logarithmic value of $IC_{50}$). For the chiral ligands studied as racemates, the same affinity was attributed to both enantiomers. This assumption was necessary in the absence of information on the binding stereoselectivity to the separate AAG variants. The effects of this assumption on CoMFA results are discussed separately for each variant (see below).

**Technical specification.** All molecular modeling calculations were performed with the Sybyl software (ver. 6.3; Tripos Associates, St. Louis, MO) running on Silicon Graphics Indy R4400 and $O_2$ R5000 workstations. Ligand starting geometries were built in their neutral form by the Concord algorithm (Tripos Associates). Energy minimization was performed with the Tripos force field including the electrostatic energy term calculated using Gasteiger and Marsili (1980) atomic charges. The method of Powell was used for minimizations, with convergence being reached when the gradient decrease was <0.001 kcal/mol/Å. The DISCO module of Sybyl was used in combination with quenched molecular dynamics as described previously (Caron *et al.*, 1997).

For the CoMFA studies, the QSAR module of Sybyl was used with the three molecular fields (steric, electrostatic, and lipophilic). The lipophilicity field was calculated by the molecular lipophilicity potential (Gaillard *et al.*, 1994). The specific parameters used for CoMFA include a grid size of 1.5 Å and atomic charges calculated with the Gasteiger and Marsili (1980) approach.

The three-dimensional matrix generated (affinity as dependent variable and molecular field value in each grid point as independent variable) was analyzed by SAMPLS (Bush and Nachbar, 1993) (PLS cross-validation with minimum $\sigma = 2$) to retain models with $q^2 > 0.4$ (Gaillard *et al.*, 1994). For PLS analyses, the leave-one-out procedure was chosen for cross-validation. The number of principal components (N) in the final PLS analysis was determined on the basis of the empirical rule that allows a component to be retained if it increases the predictive power of the model ($q^2$) by ~10% relative to the previous component. As discussed later, a careful investigation of the graph $q^2 = f(N)$ was the crucial step to select the models to be submitted to the final PLS analyses (PLS cross-validation with minimum $\sigma = 0$). The other options were chosen according to published standards (Simon, 1992; Folkers *et al.*, 1993).

**Alignment of ligands.** For the A variant, manual ligand alignments were performed using the optimized geometries modified by manual geometrical fitting. All molecules were aligned on the template amitriptyline. Amitriptyline was chosen because it was the most rigid among compounds with high binding affinity. The geometry of the template was optimized by energy minimization.

The alignment of ligands was based on their aromatic moieties (often two) and basic nitrogen: (1) the aromatic moieties were aligned by their centroid and the normal to their plane, and (2) the free-electron lone pairs of the basic nitrogen were pointed in the same direction. Due to their small structural similarity with other ligands, diazepam and progesterone could not be aligned satisfactorily and had to be excluded from the CoMFA study.

For the F1*S variants, the DISCO approach was used to find alignments (Martin *et al.*, 1993; Myers *et al.*, 1994), which were then submitted to SAMPLS.

### Presentation of Results

The graphic results present the most relevant regions of space where the variations of a chosen statistical field are the largest. In each grid point, a statistical field is defined as the product of its coefficient in the PLS equation by the standard deviation.

## Results

### Ligand Displacement Studies

The results of the displacement of [$^3$H]imipramine bound to the A variant and of [$^{14}$C]warfarin bound to the F1*S variant mixture showed that the displacing ligands displayed very different inhibitory potencies. Examples of displacement of imipramine from the A variant and of warfarin from the F1*S variants are shown in Figs. 1, A and B, respectively. The theoretical curves representing a competitive inhibition of the marker binding fitted the data well, with a few exceptions discussed below. The $IC_{50}$ values of the ligands calculated from the displacement curves are listed in Table 1. The values were in the range of 5.6 $\mu$M (**11**, propafenone) to 673 $\mu$M (**32**, minaprine) for [$^3$H]imipramine binding to the A variant and in the range of 5.0 $\mu$M (**31**, thioridazine) to 814 $\mu$M (**22**, desipramine) for [$^{14}$C]warfarin binding to the F1*S variants.

Amitriptyline, a tricyclic antidepressant drug (**19**; $IC_{50}$ = 6.1 $\mu$M), was one of the most potent displacers of [$^3$H]imipramine. The tricyclic antidepressants as a group (compounds **19** and **21**-**26**) were potent displacers of imipramine but had poor or no inhibitory potency toward warfarin (Table 1). Several antihistaminic drugs (compounds **4**, **6**, and **7**) also seemed to displace preferentially imipramine bound to the A variant. In contrast, other ligands, such as $\beta$ blockers (compounds **14**-**16**; see Table 1), had comparable inhibitory potencies for the A and F1*S variants. Plotting the ligand inhibitory potencies to F1*S variants versus those to the A variant revealed the absence of any correlation between these two sets of data (result not shown).

A few drugs did not inhibit competitively the binding of the marker (Table 1). The small displacement of bound radiomarker measured after the addition of these drugs (i.e., the percentage of displacement did not exceed 16 ± 6% at the highest inhibitor concentrations) (data not shown) was assigned to nonspecific binding.

To compare further the binding specificities of the A and F1*S variants, the binding association constants ($K'$) of the inhibitors were calculated from the displacement data using a model for competitive binding at varying numbers of iden-

Downloaded from molpharm.aspetjournals.org at ASPET Journals on November 19, 2017

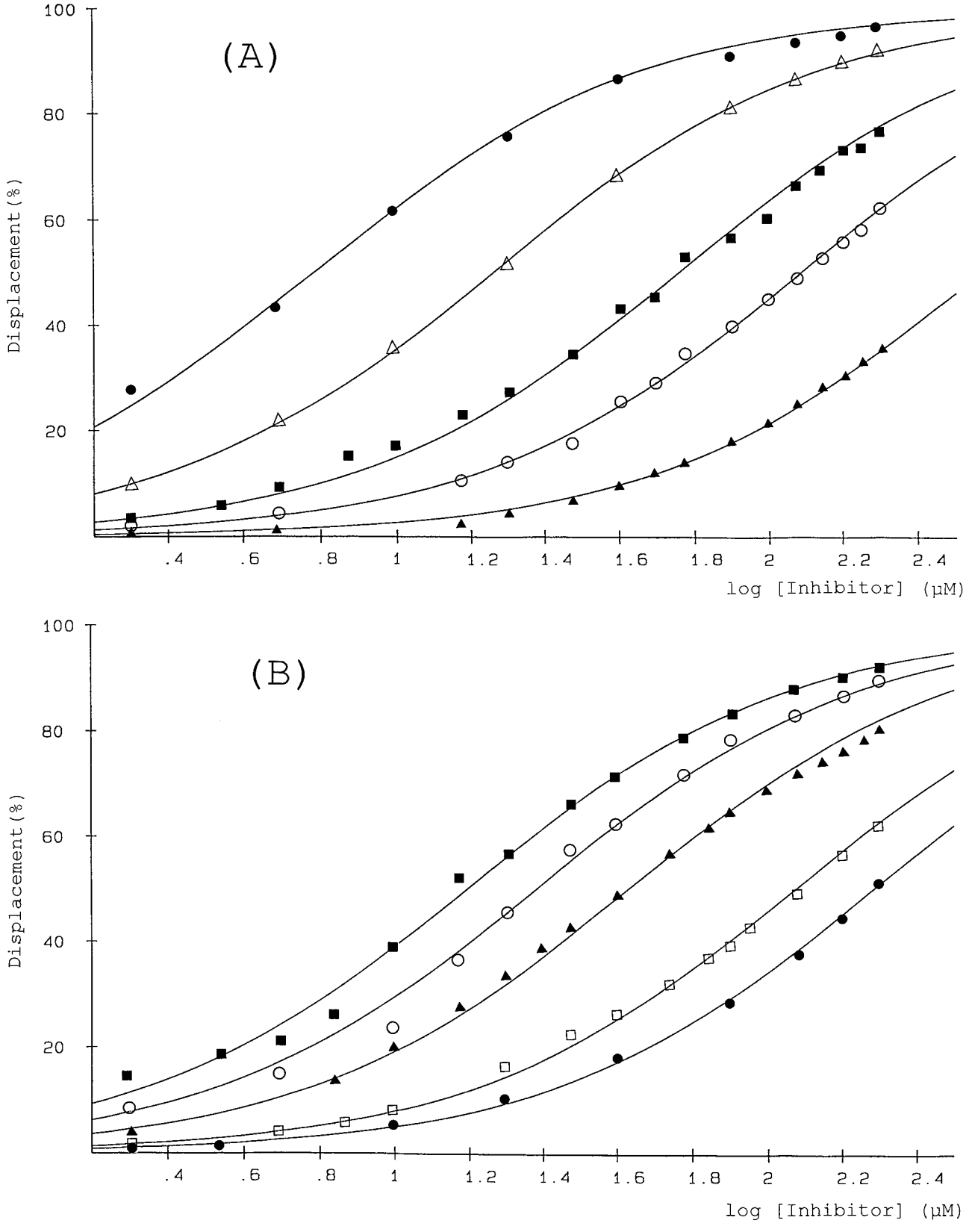


**Fig. 1.** Examples of displacement of [$^3$H]imipramine from the A variant (A) and of [$^{14}$C]warfarin from the F1*S variants (B) by the addition of various ligands. Displacers used were amitriptyline (●), promethazine (△), propranolol (■), chlorcyclizine (○), and viloxazine (▲) in A and tertatolol (■), isradipine (○), propafenone (▲), prazosin (□), and amitriptyline (●) in B. The mean data from two or three triplicate displacement experiments are shown. The coefficients of variation of the data were between 0.9% and 27.7% for [$^3$H]imipramine and the A variant and between 0.1% and 26.0% for [$^{14}$C]warfarin and the F1*S variants. *Solid lines*, theoretical displacement curves representing a competitive inhibition of the marker binding by displacer.

Downloaded from molpharm.aspetjournals.org at ASPET Journals on November 19, 2017

tical protein sites (see Experimental Procedures). The calculated values of $K'$ are shown in Table 1. This table also shows a selectivity factor (S), namely the ratio of affinities of a ligand for the A variant to those for the F1*S variants. The values of $K'$ ranged from $4.18 \times 10^6$ liter/mol (**11**, propafenone) to $0.015 \times 10^6$ liter/mol (**32**, minaprine) for the A variant and from $6.00 \times 10^6$ liter/mol (**31**, thioridazine) to $0.018 \times 10^6$ liter/mol (**22**, desipramine) for the F1*S variants. It is of interest to note that the ranking of the ligands according to the values of $K'$ in Table 1 closely parallels the ranking according to the $IC_{50}$ values. Furthermore, back-calculation from the binding parameters and total reagent concentrations gave theoretical marker ligand displacements that correlated closely with the experimental values ($r > 0.95$), showing that the model used was able to account for the experimental results. The only exceptions concerned the few low affinity ligands indicated in Table 1.

### CoMFA

**A variant.** A number of alignments of ligands were tested. The alignment shown in Fig. 2 was retained for the final analyses because it afforded the best statistical results and the best superposition of haptophoric elements. The many CoMFA models obtained were compared by means of a plot of $q^2$ versus N (Fig. 3). This indispensable procedure identified the best CoMFA models to be submitted to final PLS analysis. As shown in Fig. 3, the electrostatic field was poorly correlated with affinity and decreased $q^2$ when combined with other fields. The final model therefore was free from electrostatic contributions. The lipophilic field alone gave no model with $q^2 > 0.4$ and even lowered the $q^2$ of the steric field alone when combined with it. This led us to believe that the variability in affinity is explainable mainly by steric properties of the ligands. However, and according to general CoMFA rules, a final analysis was performed for all models with a value of $q^2 > 0.4$. To avoid possible artifacts due to the mixing of several molecular fields, the lipophilic model also was submitted to a final analysis.

Thus, three models were retained. Their statistical values after final PLS analysis are reported in Table 2. Clearly, model 1 (steric field only) is the best one, with a $q^2$ of 0.57 and an $r^2$ of 0.953. Its graphic representation and interpretation are discussed.

**F1*S variants.** Should the F1*S variants be characterized by a single binding mode different from that of the A variant, a CoMFA alignment successful in modeling binding to the A variant would fail for the F1*S variants? This was tested with the manual alignment that was successful for the A variant used for the F1*S binding data (i.e., steric model 1). No model with $q^2 > 0.4$ was obtained.

The DISCO approach was used to find other alignments (Martin *et al.*, 1993; Myers *et al.*, 1994). These were submitted to SAMPLS, yielding hundreds of models, with each having three hydrophobic features and no basic center. These models were all very similar and differed only in the conformation of one or two ligands. Some models were arbitrarily retained, and the major inconsistencies were corrected manually (e.g., ligands with similar structural features should have the same orientation). No model with $q^2 > 0.4$ was found.

## Discussion

### Binding Studies

Our previous studies with smaller sets of ligands have demonstrated differences and similarities in the ligand-bind-

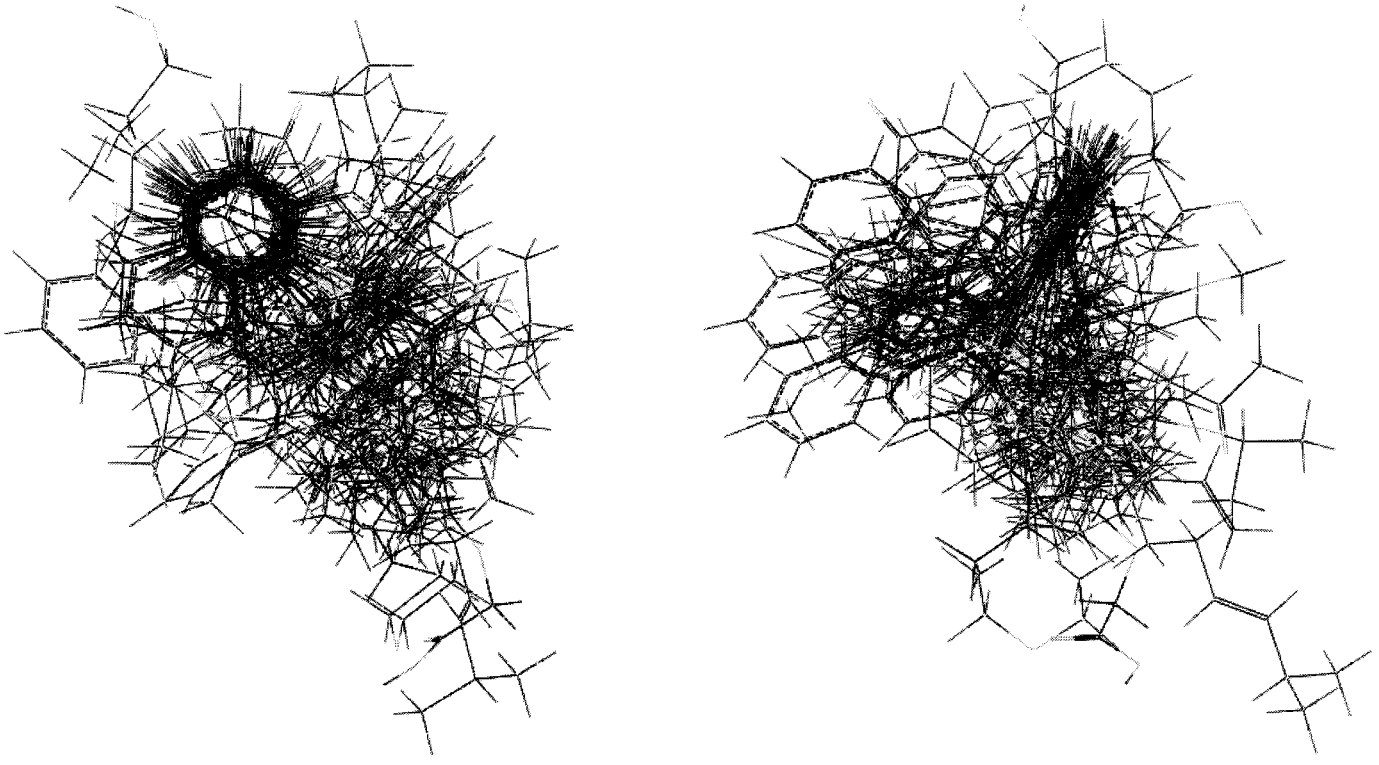

**Fig. 2.** Two projections (90-degree rotation) of the final alignment of ligands of the A variant.

Downloaded from molpharm.aspetjournals.org at ASPET Journals on November 19, 2017

ing properties of the A and F1*S variants (i.e., the two main *AAG* gene products) (Hervé *et al*., 1993b, 1996). The results presented here both extend the knowledge of the AAG variants binding properties and allowed us to model the high affinity site of the A variant.

Although the $IC_{50}$ values calculated here are independent of the binding model, the $K'$ values and the site modeling assume competitive binding at a single-site class with insignificant nonspecific binding. This is justified on several grounds. Theoretical calculations from known binding parameters for both high and low affinity sites showed that under the conditions used here, <6% of the binding of marker ligand would be at the low affinity sites. The good correlation between the experimentally determined displacements and theoretical marker ligand displacements back-calculated from the binding parameters and total reagent concentrations demonstrated that the model adequately fitted the experimental results. Further evidence for the validity of the model is shown by the parallel ranking of the inhibitor $K'$ and (model-independent) $IC_{50}$ values. Also, previous binding studies with some of the ligands used here as inhibitors (i.e., compounds **1**, **9**, **10**, **18**, **30**, and **33** described in Table 1) showed that the stochiometry of the interactions between the A and the F1*S variants with their respective specific ligands was ~1, suggesting that these ligands share a single common binding site on each of these variants (Hervé *et al*., 1996). Furthermore, the association constants ($K'$) estimated for these ligands from the displacement experiments based on the assumption of competitive inhibition were comparable to the association constants ($K_a$) determined in the direct binding studies. For the current work, the direct binding of (radiolabeled) propranolol also was determined (data not shown), and it gave association constants close to the $K'$ values in Table 1 ($K_a$ = 0.22 and 0.21 × $10^6$ liter/mol for the A and F1*S variants, respectively).

The current results allow insight into the nature and topography of the binding site or sites likely to be present on each AAG variant. Using a large number of medicinal ligands, we bring evidence that the drugs with selective affinity for the A variant share marked structural similarities, most of them containing a basic amino group linked by a short carbon chain to two aromatic rings that are either bridged to form a tricyclic structure (e.g., amitriptyline, nortriptyline, imipramine, desipramine, maprotiline, and promethazine) or unbridged (e.g., disopyramide, methadone, and diphenhydramine). However, other analogues of imipramine (e.g., clomipramine and desmethylclomipramine) or diphenhydramine (e.g., chlorcyclizine, cetirizine, and chlorpheniramine) or promethazine (e.g., chlorpromazine) had little or no selectivity for the A variant.

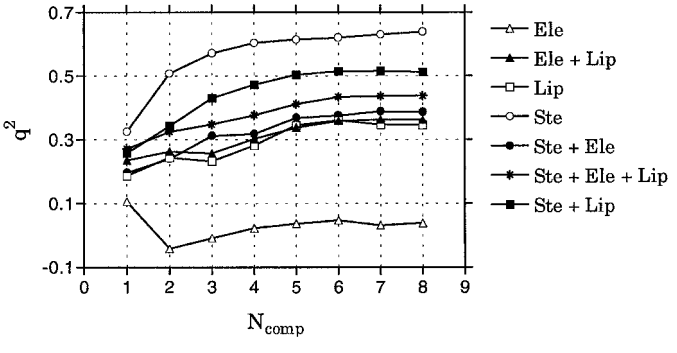


**Fig. 3.** Plot of $q^2$ versus N (the number of components): final PLS analysis was performed for all models with a value of $q^2 > 0.4$. *Ste*, steric field; *ele*, electrostatic field; *lip*, lipophilic field.

These results suggest that substitution of an aromatic ring with a chlorine atom or the presence of a piperidine ring may be factors leading to decreased ligand binding selectivity to the A variant. These findings indeed are made explicit by the CoMFA model (see below).

In contrast, no clear analogies were found for the selective ligands of the F1*S variants (e.g., dipyridamole, warfarin, binedaline, and prazosin), except for a relatively large hydrophobic ring system (Hervé *et al*., 1996). This suggests that the ligand binding site of the F1 and S variants could be a relatively large hydrophobic pocket able to accommodate a variety of chemical structures, whereas the A variant binding site seems to be of smaller size and of greater ligand specificity. In addition, the A and F1*S variants display similar affinities for a variety of other ligands, suggesting that these share some common structural features or physicochemical properties with other ligands selectively bound by the A or F1*S variants. This preliminary hypothesis then was challenged by a 3D-QSAR study using the CoMFA approach.

## CoMFA

**Graphic representation of the model for the A variant.** The graphic results of the best CoMFA model obtained (Table 2, model 1) are represented in Fig. 4 with (*R*)-bornaprolol (a high affinity ligand) in position and in Fig. 5 with minaprine (a low-affinity ligand) in position. A number of sterically unfavorable regions (*dark gray*) can be seen located around and below the aromatic ring R1 (Fig. 5A) and below the basic nitrogen (Fig. 5B), indicating forbidden positions. In contrast, there are favorable influences (*light gray*) above the second ring R2 (Fig. 5C) and behind the basic nitrogen (Fig. 5D). This is reasonable given that (1) zone A was deduced from the low affinity of compounds containing a chlorine atom as substituent in the aromatic ring, (2) zone B explains the low affinity of ligands containing a piperidine ring, (3) zone C was deduced from the relative orientation of the two rings present in high affinity tricyclic drugs, and (4) zone D explains the high affinity of *N*-methylated amines.

When examining the binding modes of a high affinity and a low affinity ligand, it seems that (*R*)-bornaprolol fits well in the light-gray regions and escapes forbidden dark-gray regions (Fig. 4), whereas the opposite is true for minaprine (Fig. 5).

This model therefore is able to explain the variation in

TABLE 2
Statistics for CoMFA models

| Model | Field type[a] | $q^2$ [b] | N[c] | $r^2$ [d] | s[e] | F[f] | ste[g] | lip[h] |
|---|---|---|---|---|---|---|---|---|
| 1 | ste | 0.57 | 3 | 0.953 | 0.147 | 263 | 100 | |
| 2 | lip | 0.34 | 5 | 0.964 | 0.132 | 198 | | 100 |
| 3 | ste and lip | 0.47 | 4 | 0.967 | 0.124 | 282 | 41.9 | 58.1 |

[a] Molecular field(s) used in CoMFA: ste, steric field; ele, electrostatic field; lip, lipophilic field.
[b] Cross-validation correlation coefficient.
[c] Number of components used in final PLS analyses (see text).
[d] Correlation coefficient of the final PLS analysis.
[e] Standard error of estimate, measure of the unexplained uncertainty.
[f] F ratio: the higher the F ratio, the better the PLS analysis.
[g] Relative contribution of the steric (ste) and lipophilic (lip) fields in the final PLS analysis.

Downloaded from molpharm.aspetjournals.org at ASPET Journals on November 19, 2017

selectivity of some analogues of imipramine for the A variant. In fact, the presence of one or more groups in forbidden positions modulates the selectivity of these drugs with similar chemical structure for the variant.

Based on the graphic results of the steric model 1 (Figs. 4 and 5), a simplified haptophoric model can be proposed (Fig. 6), showing the moieties and intramolecular distances that are favorable for binding to the A variant. These moieties are a basic nitrogen atom, a ring (R1) binding in a hydrophobic pocket, and another ring (R2) interacting with a hydrophobic area. The validity of the model does not seem to be affected by a lack of information on the enantioselectivity of some of the ligands. In line with this, previous investigators have reported small differences among the individual enantiomers of disopyramide (Lima *et al.*, 1984; Brunner and Müller, 1987), methadone (Eap *et al.*, 1990), and propafenone (Volz *et al.*, 1994) for binding to purified or plasma AAG. Because these drugs are bound selectively by the A variant of AAG (Hervé *et al.*, 1996; current study), small differences for binding to the A variant also should exist among their respective enantiomers.

Model 2 generated by the lipophilicity field alone (Table 2) is below the level of statistical significance. Model 3 (Table 2), which contains the steric and lipophilicity fields, also is statistically acceptable, but its graphic results (figure not shown) reveal fragmented zones that are difficult to interpret.

**F1*S variants.** The impossibility of finding a statistically acceptable ($q^2 > 0.4$) 3D-QSAR model for binding to the F1*S variants using the same alignment as for the A variant

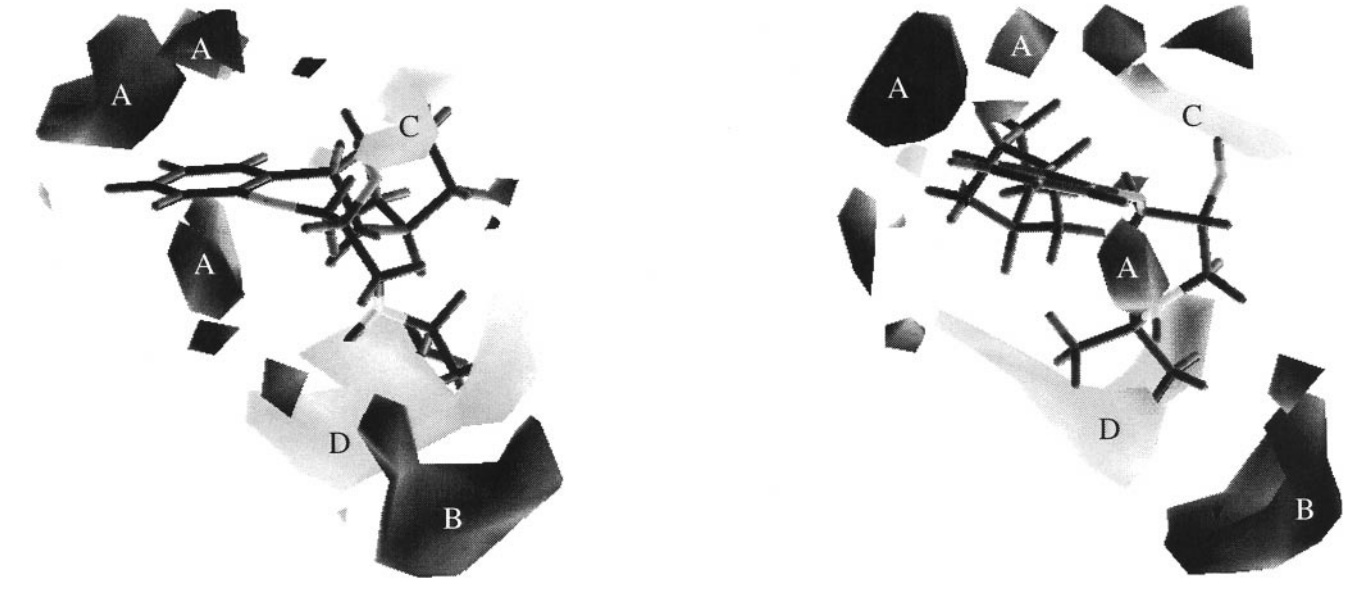


**Fig. 4.** Two projections (90-degree rotation) of the PLS model 1 for the A variant, with the high affinity ligand (*R*)-bornaprolol in position. *Light gray*, favorable steric influences. *Dark gray*, unfavorable steric influences.

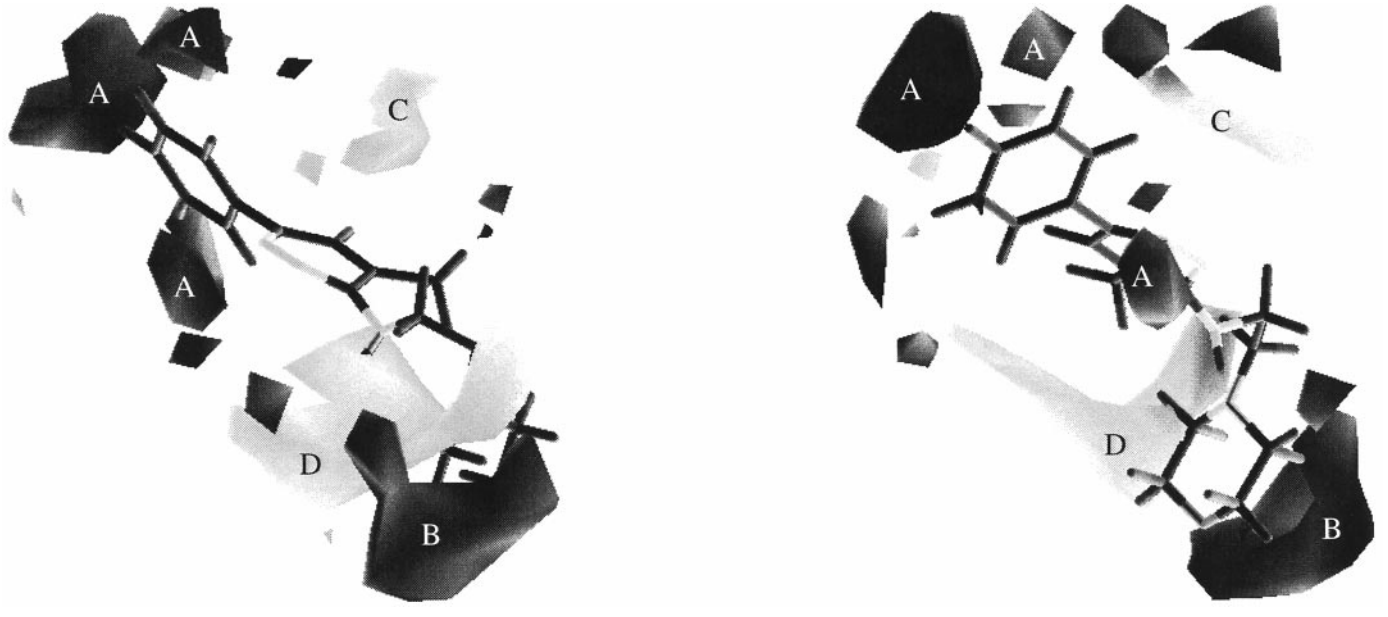


**Fig. 5.** Two projections (90-degree rotation) of the PLS model 1 for the A variant, with the low-affinity ligand minaprine in position. *Light gray*, favorable steric influences. *Dark gray*, unfavorable steric influences.

Downloaded from molpharm.aspetjournals.org at ASPET Journals on November 19, 2017

confirms that their binding site is different from that of the A variant, as found by Raes *et al*. (1987). Furthermore, the fact that no other alignment gave a 3D-QSAR model suggests a number of different, partly incompatible explanations. The first is that the F1 and S variants have different binding sites and that the experimental affinity data are composite values. However, the existence of both a high degree of primary sequence homology (Dente *et al*., 1987) and similar ligand binding properties between the individual F1 and S variants (Hervé *et al*., 1993a and 1993b) does not support this hypothesis.

The second hypothesis is that the F1 and S variants have an identical and adaptable binding site that allows different, topographically incongruent binding modes. This last explanation is in better agreement with a previous hypothesis (Hervé *et al*., 1996) and with the current experimental data, which suggest this site to be a large hydrophobic area with no obvious structural requisites for binding. In particular, a basic moiety clearly is not mandatory for binding.

Third, [$^{14}$C]warfarin was used as a selective and high affinity ligand for the F1*S variants in the displacement studies. A fractional number of high affinity sites ($n_1$ = 0.58) had previously been determined for the binding of warfarin to the F1*S mixture (Hervé *et al*., 1993b). This small number of sites was not due to differences between the binding properties of the two variants with respect to warfarin because these have been shown to be similar (Hervé *et al*., 1993b). Rather, it has been suggested that both F1 and S variants would bind selectively only one enantiomer of warfarin. Despite this enantioselectivity, the same affinity was attributed to both enantiomers of warfarin for the CoMFA study because it is not yet known which of the two enantiomers is stereospecifically recognized by the F1*S variants. This approximation can affect the CoMFA results, also explaining why no sound 3D-QSAR model was found for the F1*S variants. Further work is necessary to investigate the effects of the enantioselectivity of warfarin on the CoMFA results (i.e., identification of the warfarin enantiomer that is selectively bound by the F1*S variants and tests of other alignments of ligands using the appropriate enantiomer as template).

The last hypothesis is simply a paucity of adequate experimental data, with the set of ligands with high affinity for the F1*S variants lacking structural diversity.

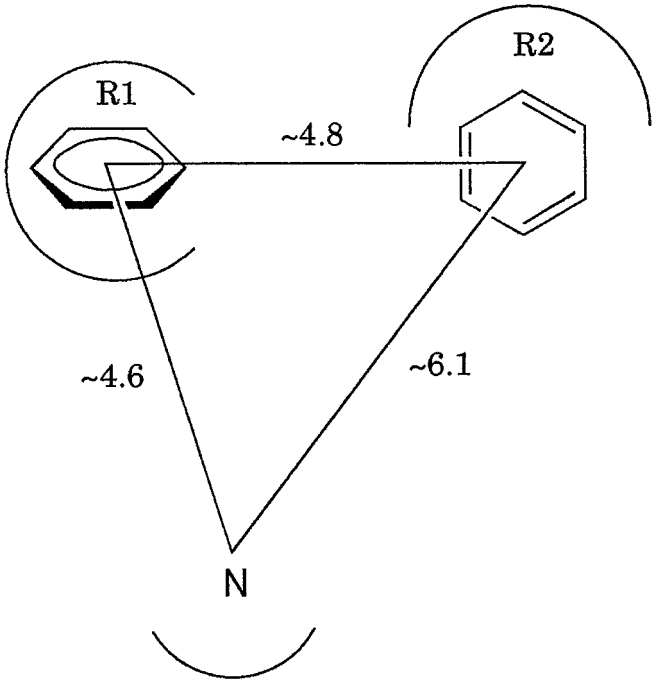


**Fig. 6.** Schematic topographical representation of the moieties and intramolecular distances (in Å) favorable for binding to the A variant. These haptophoric elements are a basic nitrogen atom, a ring (R1) binding in a hydrophobic pocket, and another ring (R2) interacting with a hydrophobic area.

## Conclusion

To the best of our knowledge, this study represents the first successful attempt to generate a homogeneous, large set of data on the binding of drugs to variants of a transport macromolecule and to obtain a 3D-QSAR model from some of these data. Until the three-dimensional structure of the AAG variants is revealed through direct investigations (e.g., NMR or X-ray crystallography), the CoMFA approach is one the best tools available to obtain indirect information on binding sites. The results reported here add to our fundamental knowledge of AAG variants, and they may well be of clinical significance given the genetic polymorphism existing for AAG in humans (Schmid, 1975; Dente *et al*., 1987; Yuasa *et al*., 1993) and the clear importance of this protein in the plasma binding of drugs (Routledge, 1986).

### References

Brunner F and Müller WE (1987) The stereoselectivity of the 'single drug binding site' of human *alpha*-1-acid glycoprotein (orosomucoid). *J Pharm Pharmacol* **39:** 986–990.

Bush BL and Nachbar RB Jr (1993) Sample-distance partial least squares: PLS optimized for many variables, with application to CoMFA. *J Comput Aided Mol Design* **7:**587–619.

Caron G, Gaillard P, Carrupt PA, and Testa B (1997) Lipophilicity behavior of model and medicinal compounds containing a sulfide, sulfoxide, or sulfone moiety. *Helv Chim Acta* **80:**449–462.

Dente L, Pizza MG, Metspalu A, and Cortese R (1987) Structure and expression of the genes coding for human *alpha*-1-acid glycoprotein. *EMBO J* **6:**2289–2296.

Eap CB and Baumann P (1988) Isoelectric focusing of *alpha*-1-acid glycoprotein (orosomucoid) in immobilized pH gradients with 8 M urea: detection of its desialylated variants using an alkaline phosphatase-linked secondary antibody system. *Electrophoresis* **9:**650–654.

Eap CB and Baumann P (1989) The genetic polymorphism of human alpha-1-acid glycoprotein, in *Alpha-1-Acid Glycoprotein. Genetics, Biochemistry, Physiological Functions and Pharmacology* (Baumann P, Eap CB, Müller WE, and Tillement JP, eds) pp 111–125, Alan R. Liss, New York.

Eap CB, Cuendet C, and Baumann P (1990) Binding of *d*-methadone, *l*-methadone and *dl*-methadone to proteins in plasma of healthy volunteers: role of the variants of *alpha*-1-acid glycoprotein. *Clin Pharmacol Ther* **47:**338–346.

Eap CB, Fischer JF, and Baumann P (1991) Variations in relative concentrations of variants of human *alpha*-1-acid glycoprotein after acute-phase conditions. *Clin Chim Acta* **203:**379–386.

Folkers G, Merz A, and Rognan D (1993) CoMFA: scope and limitations, in *3D QSAR in Drug Design: Theory Methods and Applications*. (Kubinyi H, ed) pp 583–618, ESCOM Science Publishers, Leiden.

Gaillard P, Carrupt PA, Testa B, and Boudon A (1994) Molecular lipophilicity potential, a tool in 3D-QSAR: method and applications. *J Comput Aided Mol Design* **8:**83–96.

Gasteiger J and Marsili M (1980) Iterative partial equalization of orbital electronegativity: a rapid access to atomic charges. *Tetrahedron* **36:**3219–3222.

Hervé F, Duché JC, Barré J, Millot MC, and Tillement JP (1992) pH titration curves of the desialylated human *alpha*-1-acid glycoprotein variants by combined isoelectrofocusing-electrophoresis: utilization in the development of a fractionation method for the protein variants by chromatography on immobilized metal affinity adsorbent. *J Chromatogr* **577:**43–59.

Hervé F, Duché JC, d'Athis P, Marché C, Barré J, and Tillement JP (1996) Binding of disopyramide, methadone, dipyridamole, chlorpromazine, lignocaine and progesterone to the two main genetic variants of human $\alpha_1$-acid glycoprotein: evidence for drug-binding differences between the variants and for the presence of two separate drug-binding sites on $\alpha_1$-acid glycoprotein. *Pharmacogenetics* **6:**403–415.

Hervé F, Fouache F, Marché C, and Tillement JP (1997) Abnormal microheterogeneity detected in one commercial $\alpha$1-acid glycoprotein preparation using chromatography on immobilized metal affinity absorbent and on hydroxyapatite. *J Chromatogr B* **688:**35–46.

Hervé F, Gomas E, Duché JC, and Tillement JP (1993a) Fractionation of the genetic variants of human $\alpha_1$-acid glycoprotein in the native form by chromatography on an immobilized copper(II) affinity absorbent: heterogeneity of the separate vari-

Downloaded from molpharm.aspetjournals.org at ASPET Journals on November 19, 2017

ants by isoelectrofocusing and by concanavalin A affinity chromatography. *J Chromatogr* **615:**47–57.
Hervé F, Gomas E, Duché JC, and Tillement JP (1993b) Evidence for differences in the binding of drugs to the two main genetic variants of human *alpha*-1-acid glycoprotein. *Br J Clin Pharmacol* **36:**241–249.
Kremer JMH, Wilting J, and Janssen LMH (1988) Drug binding to human *alpha*-1-acid glycoprotein in health and disease. *Pharmacol Rev* **40:**1–47.
Lima JL, Jungbluth GL, Devine T, and Robertson LW (1984) Stereoselective binding of disopyramide to human plasma proteins. *Life Sci* **35:**835–839.
Martin YC, Bures MG, Danaher EA, DeLazzer J, Lico I, and Pavlik PA (1993) A fast new approach to pharmacophore mapping and its application to dopaminergic and benzodiazepine agonists. *J Comput Aided Mol Design* **7:**83–102.
Myers AM, Charifson PS, Owens CE, Kula NS, McPhail AT, Baldessarini RJ, Booth RG, and Wyrick SD (1994) Conformational analysis, pharmacophore identification, and comparative molecular field analysis of ligands for neuromodulatory $\sigma_3$ receptor. *J Med Chem* **37:**4109–4117.
Raes M, Michiels C, and Remacle J (1987) Comparative study of the enzymatic defense systems against oxygen derived free radicals: the key role of glutathione peroxidase. *Free Rad Biol Med* **3:**3–7.
Routledge PA (1986) The plasma protein binding of basic drugs. *Br J Clin Pharmacol* **22:**499–506.
Schmid K (1975) *Alpha*-1-acid glycoprotein, in *The Plasma Proteins: Structure, Function and Genetic Control* (Putnam FW, ed) pp 183–228, Academic Press, New York.
Simon Z (1992) Comparative molecular field analysis: critical comments. *Rev Roum Chimie* **37:**323–325.
Tinguely D, Baumann P, Conti M, Jonzier-Perey M, and Schöpf J (1985) Inter-individual differences in the binding of antidepressants to plasma proteins: the role of the variants of *alpha*-1-acid glycoprotein. *Eur J Clin Pharmacol* **27:**661–666.
Tomei L, Eap CB, Baumann P, and Dente L (1989) Use of transgenic mice for the characterization of human $\alpha_1$-acid glycoprotein (orosomucoid) variants. *Hum Genet* **84:**89–91.
Volz M, Mitrovic V, and Schlepper M (1994) Steady-state plasma concentrations of propafenone: chirality and metabolism. *Int J Clin Pharmacol Ther* **32:**370–375.
Yuasa I, Weidinger S, Umetsu K, Suenaga K, Ishimoto G, Eap CB, Duché JC, and Baumann P (1993) Orosomucoid system: 17 additional orosomucoid variants and proposal of a new nomenclature. *Vox Sang* **64:**47–55.

**Send reprint requests to:** Prof. Bernard Testa, School of Pharmacy, BEP, University of Lausanne, CH-1015 Lausanne, Switzerland. E-mail: bernard.testa@ict.unil.ch

Downloaded from molpharm.aspetjournals.org at ASPET Journals on November 19, 2017